Presented at the 20th European Photovoltaic Solar Energy Conference and Exhibition,
Barcelona, Spain, 6-10 June 2005

MODELLING OF LUMINESCENT CONCENTRATORS BY RAY-TRACING

A.R. Burgers, L.H. Slooff, R. Kinderman, J.A.M. van Roosmalen.
Energy research Centre of the Netherlands, P.O.Box 1, NL-1755 ZG Petten, The Netherlands
tel: +31 224 564959, fax: +31 224 56 8214, email: burgers@ecn.nl

ABSTRACT: We have made luminescent concentrator devices by gluing multi-crystalline silicon solar cells to polymer plates containing fluorescent dyes. The devices have been characterised by optical reflection- and transmission measurements and with external quantum efficiency measurements. We have applied different mirror configurations to the devices to improve the external quantum efficiency. The measurements have been modelled with a ray-tracing simulation. The simulation allows us to analyse loss mechanisms in the device.
keywords: concentrator, photoluminescense, simulation.

1 INTRODUCTION

An interesting approach for conversion of light to electricity is the luminescent flat plate concentrator [1,2]. It consists of a transparent flat plate with solar cells connected to one or more sides (See Figure 1). The plate contains luminescent particles such as organic dyes or quantum dots that absorb the light and re-emit part of the absorbed light diffusely at a longer wavelength.

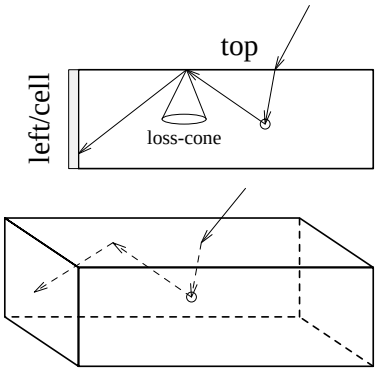

Figure 1: the luminescent concentrator: incident light is absorbed and re-emitted diffusely by luminescent particles in the polymer plate. The emitted light is transported to a solar cell at the left, the polymer plate acting as a wave guide.

Part of the diffuse luminescence of these particles is guided through the plate by total internal reflection to solar cells fitted at the edges, the plate functioning as a wave guide. The device hence allows concentration of light entering the top surface onto a small photoactive area at the edge of the concentrator.

The luminescent concentrator has several potential advantages. One advantage is that it operates both on incident diffuse light and on direct light. A second advantage is that it might result in cost reduction of photovoltaic energy by concentrating light. For further development and improvement of the luminescent concentrator it is important to understand the loss mechanisms.

2 APPROACH

Luminescent concentrator devices have been prepared. The devices have been characterized by optical reflection- and transmission measurements and external quantum efficiency measurements. Subsequently ray-tracing modelling was done to analyse these measurements.

2.1 Sample preparation

Luminescent concentrator devices were assembled at ECN. In the paper by Slooff [3] in these proceedings the details of the device processing can found.

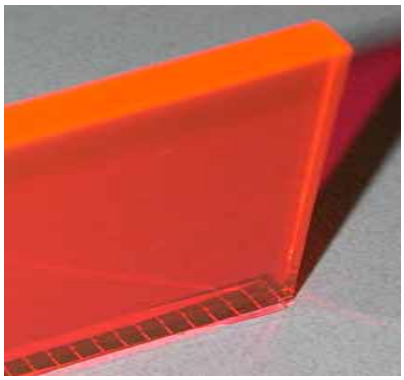

Figure 2: a multi-crystalline silicon solar cell fitted to a polymer slab.

In Figure 2 a photograph of a multi-crystalline silicon solar cell fitted to a polymer slab is shown. The polymer slab measures 50x50x5 mm^3, the cell measures 50x5 mm^2. This geometry allows for a geometrical concentration of a factor 10. This is the ratio between the areas of the light receiving top surface and the cell. The Plexit polymer slabs have been prepared at the Fraunhofer Institute for Applied Polymer Research in Potsdam (Germany). The dye used was Fluorescent red G, a coumarin derivative supplied by Bayer. The multi-crystalline silicon solar cells were laser cut from cells manufactured in the ECN pilotline.

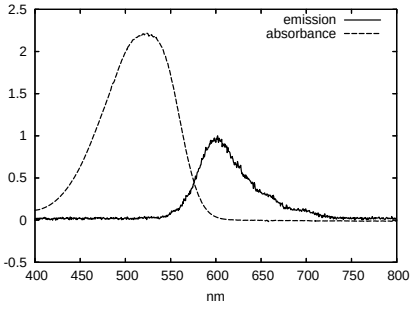

Figure 3: absorption and emission of dye Fluorescent red

In Figure 3, the absorption and emission characteristics of this dye are shown.

2.2 Reflection- and transmission measurements

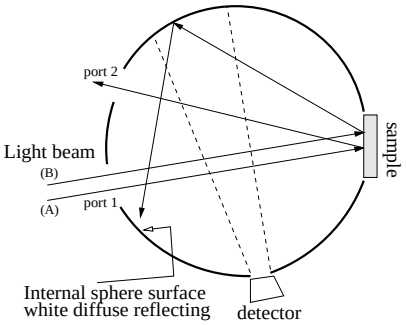

Figure 4: Integrating sphere layout for reflection measurements.

The optical measurements on the polymer sheets were done with the help of an integrating sphere setup (See Figure 4). In this setup, a beam of white light enters through port 1 and impinges on the sample, where part of it is reflected. Specularly reflected light hits port 2 on the sphere. In normal use, port 2 is closed with a white plug. When port 2 is open, the light that is specularly reflected by the sample (ray A in the figure) leaves the sphere. This allows to measure the light that is reflected diffusely (ray B in the figure) separately. Since the polymer plates have polished facets, diffuse reflection of the polymer faces is neglegible. As a result, light that is not absorbed by the dye leaves the device only in the specular reflection- and transmission directions. Light that is absorbed and emitted by the dye is emitted in random directions. By excluding the specular reflection component in the light by opening port 2, the emitted light can be measured separately.

A reflection measurement is calibrated by first measuring a white sample with known high reflectance. The spectrum of the light source is usually irrelevant since the reflected light has the same wavelength as the incident light. For luminescent samples this is not the case since the emitted light has a longer wavelength than the incident light. Therefore, for correct interpretation of reflection measurements of emitting samples we have to take the spectrum of the lamp into account as well.

2.3 External quantum efficiency measurements

External quantum efficiency measurements were performed on the luminescent concentrator. Details of these measurements can be found in [3]. Monochromatic light impinges perpendicularly and uniformly on the large facet of the polymer slab. The external quantum efficiency measurements were done for various mirror configurations applied to the device.

Table 1: description of mirror configurations. The cell is at the left face. The light impinges on the top interface.

abbreviation	face	
Ri	right	Al mirror at face opposite of cell.
Fr	front	Al mirror at the front face.
Re	rear	Al mirror at the rear face.
diff(85%)	bottom	Diffuse 85% mirror at the bottom interface

In Table 1 the terminology used for the different mirror configurations is explained. For instance, in Figure 8 Ri+Fr+Re means shiny aluminium mirrors at the face opposite to the cell and at the front and rear faces.

2.4 Simulation with ray-tracing

In order to analyse the measurements, we need to have a simulation of the luminescent concentrator that calculates reflection- and transmission curves and external quantum efficiency curves from a description of the device. The simulation should explain all these curves simultaneously from a single description of the device.

One approach to modelling the luminescent concentrator is the detailed balance model described by Chatten et Al.[4]. In this model the chemical potential, a function of the coordinates (x,y,z), is discretised. The chemical potentials in the cells are related to each other by the radiative transfer between the cells. A system of equations is set-up to discretise the detailed balance equations as described by Yablonovitz [1]. With this approach the complexity increases quickly with the number of cells. In order to reduce the complexity, rays travelling at different directions have to be combined. For instance, all rays within the escape cone of a particular face of the slab are combined. This restricts this approach to block shaped slabs. It also makes it difficult to take into account the dependence of the reflection coefficient on the angle of incidence at the interfaces.

Gallagher [5] has presented a ray-tracing simulation of a quantum dot based luminescent concentrator. In her approach individual quantum dots are being modelled. For accurate modelling large numbers of quantum dots (billions) need to be modelled, leading to a computationally expensive procedure.

We have chosen to employ a ray tracing procedure as well. Ray tracing for luminescent concentrators follows basic ray-tracing principles. In ray-tracing a ray represents light of a certain wavelength travelling in a certain direction. Whenever a ray can proceed in several ways, random numbers are used to determine the fate of the ray. As an example consider reflection at an interface. Suppose the reflection coefficient at the interface is 30%. A random number r is drawn from a uniform distribution in the interval [0,1]. If $r < 0.3$ we assume the ray is reflected, if $r >= 0.3$ the ray is transmitted. The main extension required is the handling of absorption/emission that is specific for the luminescent concentrator. Our 3-D program takes absorption and emission characteristics into account and handles the optical properties of metals as well as dielectrics. The reflection- and transmission coefficients at the interfaces are calculated using the matrix method. This method can be found in [6,7]. For instance, the hot-mirrors proposed by Richards et al. [8] that consist of multiple thin layers of different media can be analysed in our approach. Background absorption in host media is also handled, allowing the simulation of all optical aspects of the luminescent concentrator.

The geometry is defined by planes. For instance, a single, flat plate luminescent concentrator as shown in Figure 2 is defined by 6 planes. This is sufficient to specify the plane slabs that we are currently modelling. The ray-tracing approach also allows for easy simulation of multi-layer luminescent concentrators.

In our simulation, the situations where the progress of the ray is determined by random numbers are:

- Reflection and transmission at interfaces.
- Absorption in the polymer slab. Contrary to the approach by Gallagher we use the absorption coefficient to determine the location of absorption/emission events. When there is absorption, the intensity of light decays exponentially across the path of the ray according to

the continuous distribution $\alpha\exp(-\alpha x)$ with α the absorption coefficient and x the distance along the path of the ray.

- When a photon is absorbed and might be emitted, the quantum efficiency Q_e of the emission process is taken into account.
- When a photon is absorbed and re-emitted, it can be emitted at a range of wavelengths. A wavelength is selected from the continuous emission spectrum of the dye used (See Figure 3).
- Direction of diffuse emission. The direction of an emitted photon is not correlated to the incoming direction of the absorbed photon. The direction of the emitted ray is selected randomly from the 4π solid angle.

Reflection- and transmission curves and external quantum efficiency curves are calculated by keeping track of where the rays end. Because of the statistical nature of the ray-tracing process, large numbers of rays must be traced to obtain curves with sufficiently small noise.

3 RESULTS

3.1 Analysis of optical measurements

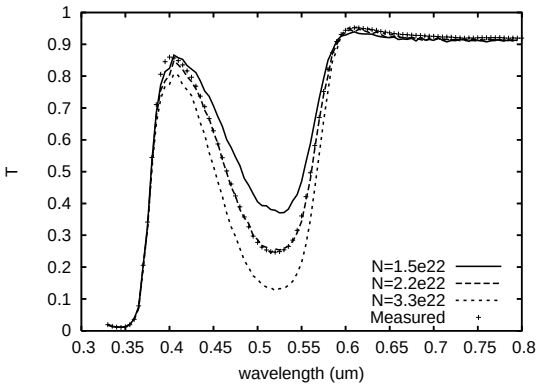

Figure 5: A measured transmission curve with 3 calculated transmission curves.

For the dye Fluorescent Red G we know the absorption cross-section as a function of wavelength (From Figure 3). The absorption coefficient of the dye is the product of the concentration of the dye and the absorption cross-section. By calculating the transmission curves for different concentrations of the dye and comparing the absorption peak between calculated and measured curves (See Figure 5), we are able to determine the concentration of the dye at 2.2 $10^{22}m^{-3}$.

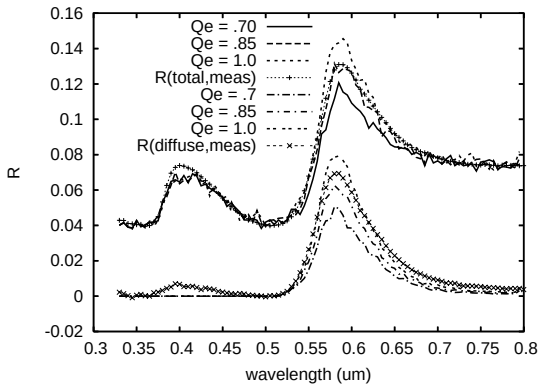

Figure 6: Measured- and calculated reflection curves.

In Figure 6 measured and calculated reflection curves are shown. Two sets of reflection curves are displayed. The set in the top of the graph has the total reflection curves, the set at the bottom has the reflection curves with the specular component omitted. The bottom set only contains the light that is diffusely reflected by the plate. Since the faces of the polymer slab are polished and scattering can be neglected, the diffusely reflected light consists only of emitted light.

We can determine the quantum efficiency of the dye by comparing the height of the emission peak at 600 nm for measured and calculated reflection curves for different values of the quantum efficiency. From this analysis we find a quantum efficiency of 85% for this dye.

The external quantum efficiency (EQE) of the device is the fraction of the incident photons that is collected by the crystalline silicon cell. Before arriving at the cell, the photons may have travelled through the polymer slab for a considerable length. Therefore the background absorption in the polymer matrix may become important [5,9]. The background absorption of Plexit polymer has been measured at Imperial College [10]. The background absorption was determined to be 4 m^{-1} in the wavelength region from 0.3-0.6 μm.

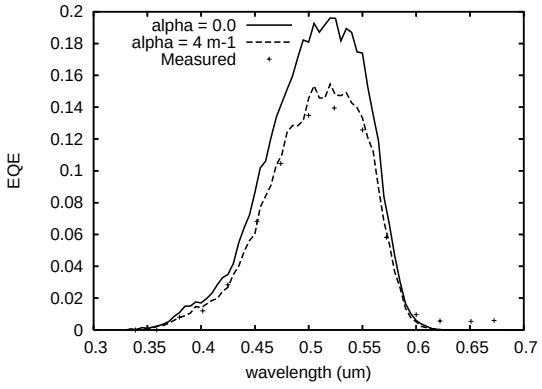

Figure 7: Influence of background absorption on calculated quantum efficiency.

From Figure 7 it is clear that the background absorption has a significant influence on the collection efficiency.

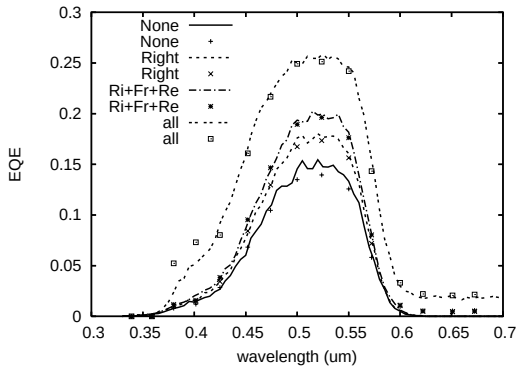

Figure 8 measured and calculated external quantum efficiency for different mirror configurations. *None* in the key means no mirrors, *all* means mirrors at all sides. Lines show the calculated EQE curves, markers show the measured ones.

In Figure 8 both the measured and calculated external quantum efficiency are shown for different mirror configurations. There is a very good agreement between calculated and measured quantum efficiency curves. Without any mirrors the device has the lowest quantum efficiency. Adding an aluminium mirror at the face opposite of the cell results in an increase in quantum efficiency. Adding mirrors at both the front and rear side in addition to the mirror at the right results in an additional increase. The biggest increase comes from adding a diffuse mirror at the bottom. Since the bottom mirror reflects diffusely, some light of the wavelengths beyond 0.6 µm will impinge on the cell without being emitted. This accounts for the EQE increase beyond .6 µm.

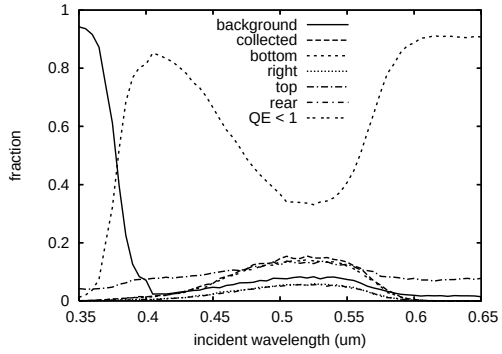

Figure 9: energy balance for the case without mirrors.

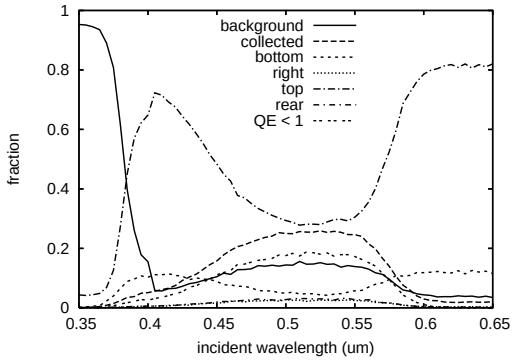

Figure 10: energy balance for the case with mirrors at Fr+Re+Ri and diffuse 85% mirror at bottom.

In Figure 9 and Figure 10, a photon balance is displayed for two different mirror configurations. Each curve shows as a function of wavelength the fraction of photons that have a certain fate. One curve for instance shows the fraction of photons that reach the solar cell. This curve corresponds to the external quantum efficiency. In the case without mirrors, the biggest loss is due to light not absorbed by the dye that escapes through the bottom. With a bottom reflector, much of this light is reflected. Some of the light will be absorbed in the reflector and more light escapes now from the top. The quantum efficiency increases because the light reflected by the bottom mirror makes an extra pass through the polymer slab and has an extra chance of being absorbed. As more light is absorbed and the dye quantum efficiency is less than 100%, the loss of photons that are absorbed but not emitted increases as well (curves labelled QE < 1). The addition of mirrors at front- and rear face leads to reduction of emitted light escaping at the front and rear faces. Some of the emitted light is absorbed in the mirrors since they do not have a perfect reflectivity.

4 CONCLUSIONS

We have described a ray-tracing simulation of luminescent concentrator devices. The simulation allows us to calculate measurable curves, such as reflection- and transmission curves and external quantum efficiency curves of luminescent devices. These curves have been measured on actual devices. By comparing measurement and simulation we are able to determine concentration and quantum efficiency of the dye. With these parameters the external quantum efficiency of the complete device can be modelled accurately. This allows us to analyse the loss-mechanisms in the device and improve these devices in the future.

[1] E. Yablonovitch, *Thermodynamics of the fluorescent planar concentrator*, J. Opt. Soc. Am., **70**, 1362-3, 1980

[2] W. Goetzberger and W. Greuble, Applied Physics, **14**, 123, 1977.

[3] L.H. Slooff et al, *The luminescent concentrator: a bright idea for spectrum conversion*, ibidem.

[4] A.J. Chatten, K.W.J. Barnham, B.F. Buxton, N.J. Ekins-Daukes and M.A. Malik, *A new approach to modelling quantum dot concentrators* Solar Energy Materials and Solar Cells, **75**, 363-71, 2004

[5] S.J. Gallagher, P.C. Eames and B. Norton, *Quantum dot solar concentrator behaviour, predicted using a ray trace approach*, Int. J. of Ambient Energy, **25**, 47-56, 2004

[6] H.A. MacLeod, *Thin Film Optical Filters*, Adam Hilger, 1986

[7] E. Hecht and A. Zajac, *Optics*, 2nd edition, Addison-Wesley, 1984,

[8] B.S. Richards, A. Shalav and R.P. Corkish, *A low escape-cone loss luminescent concentrator*, 19th EC Photovoltaic Solar Energy Conference, Paris, France, 113-116, 2004

[9] W.R.L. Thomas, J.M. Drake and M.L. Lesiecki, *Light transport in planar luminescent concentrators: the rol of matrix losses*, Applied Optics, **32**, 3440-50, 1983

[10] A.J. Chatten and D. Farrell, Imperial College, London, private correspondence, 2005